Minimum Number of 2′-*O*-(2-Aminoethyl) Residues Required for Gene Knockout Activity by Triple Helix Forming Oligonucleotides

Nitin Puri,[‡] Alokes Majumdar,[‡] Bernard Cuenoud,[§] Francois Natt,[∥] Pierre Martin,[∥] Andre Boyd,[‡] Paul S. Miller,[⊥] and Michael M. Seidman*[,‡]

Laboratory of Molecular Gerontology, National Institutes on Aging, National Institutes of Health, Baltimore, Maryland 21224, Novartis Horsham Research Centre, Horsham, West Sussex, RH12 4AB United Kingdom, Novartis Pharma, Ltd., 4002 Basel, Switzerland, and Department of Biochemistry and Molecular Biology, Bloomberg School of Public Health, Johns Hopkins University, Baltimore, Maryland 21205

Received February 26, 2002; Revised Manuscript Received March 29, 2002

ABSTRACT: Triple helix forming oligonucleotides (TFOs) that bind chromosomal targets in living cells may become tools for genome manipulation, including gene knockout, conversion, or recombination. However, triplex formation by DNA third strands, particularly those in the pyrimidine motif, requires nonphysiological pH and Mg^{2+} concentration, and this limits their development as gene-targeting reagents. Recent advances in oligonucleotide chemistry promise to solve these problems. For this study TFOs containing 2′-*O*-methoxy (2′-OMe) and 2′-*O*-(2-aminoethyl) (2′-AE) ribose substitutions in varying proportion have been constructed. The TFOs were linked to psoralen and designed to target and mutagenize a site in the hamster *HPRT* gene. T_m analyses showed that triplexes formed by these TFOs were more stable than the underlying duplex, regardless of 2′-OMe/2′-AE ratio. However, TFOs with 2′-AE residues were more stable in physiological pH than those with only 2′-OMe sugars, as a simple function of 2′-AE content. In contrast, gene knockout assays revealed a threshold requirement—TFOs with three or four 2′-AE residues were at least 10-fold more active than the TFO with two 2′-AE residues. The *HPRT* knockout frequencies with the most active TFOs were 300−400-fold above the background, whereas there was no activity against the *APRT* gene, a monitor of nonspecific mutagenesis.

The DNA triple helix has been of interest ever since its discovery more than four decades ago and the recognition that it might be exploited for manipulation of the genome (*1*−*3*). Triplexes form in a sequence-specific manner on polypurine/polypyrimidine tracts, which are abundant in mammalian genomes (*4*−*6*). The third strand of nucleic acid lies in the major groove of an intact duplex and is stabilized by Hoogsteen hydrogen bonds between third-strand bases and the purine bases in the duplex (*7*, *8*). Depending on the nature of the target sequences triplexes can be formed by third strands consisting of pyrimidines or purines, and a binding code has been described (*9*, *10*). The possibility that triple helix forming oligonucleotides (TFOs)[1] might be developed as gene-targeting reagents for application in living cells has attracted attention in recent years (*11*−*17*).

Although triplexes form on intact duplexes without any protein or enzyme requirement, biological applications are compromised by limitations imposed by the physiological environment. In particular, pyrimidine motif triplexes are unstable at physiological pH because of the requirement for cytosine protonation that occurs at a relatively acidic pH ($pK_a = 4.5$). The protonation is necessary for hydrogen bonding, and the resultant positive charge also contributes to triplex stability (*18*). Triplex formation requires relatively high levels of Mg^{2+} to neutralize the charge repulsion between the third strand and the duplex phosphates (*19*). These concentrations are higher than those thought to be available intracellularly (*20*).

Some progress toward overcoming these limitations has been achieved via the introduction of various base, sugar, and backbone modifications in TFOs. The use of 5-methylcytosine partially alleviates the pH restriction of TFOs in the pyrimidine motif (*21*, *22*), which has also been addressed with an adenine analogue (*23*). 5-Propynyldeoxyuridine reduces the Mg^{2+} dependence (*24*), as does replacement of the ribose with a morpholino analogue (*25*). The recognition that RNA third strands formed more stable pyrimidine triplexes than the corresponding DNA (*26*) prompted the introduction of 2′-*O*-methoxy (2′-OMe) sugar residues, which enhance triplex stability (*27*, *28*). The 2′,4′ bridged ribose substitution also improves triplex stability, under conditions that may be physiologically relevant (*29*). Intercalators have been linked to TFOs to improve binding (*30*), a strategy that we employed in our initial demonstration of targeted gene knockout in mammalian cells (*16*).

Backbone modifications that replace the phosphate linkage altogether (*31*), or a bridging (*32*) oxygen with a nitrogen,

* Address correspondence to this author at LMG/NIA/NIH, 5600 Nathan Shock Dr., Baltimore, MD 21224 [telephone (410) 558-8565; fax (410) 558-8157; e-mail seidmanm@grc.nia.nih.gov].

[‡] National Institutes on Aging.

[§] Novartis Horsham Research Centre.

[∥] Novartis Pharma, Ltd.

[⊥] Johns Hopkins University.

[1] Abbreviations: 2′-AE, 2′-*O*-(2-aminoethyl); 2′-OMe, 2′-*O*-methoxy; pso, psoralen; TFO, triple helix forming oligonucleotide; HPRT, hypoxanthine guanosine phosphoribosyl transferase; T_m, temperature of half-dissociation; CHO, Chinese hamster ovary.

10.1021/bi025734y CCC: $22.00
Published on Web 05/23/2002

improve TFO activity in vitro. In particular, replacement of a nonbridging oxygen in the backbone with a charged amine reduced the likelihood of self-structure formation of purine TFOs in physiological K^+ (*33*, *34*) and increased the bioactivity of a purine motif TFO (*35*). A positive charge on a thymidine analogue (*36*) or linkage of positively charged moieties to TFOs also enhance triplex stability (*37*, *38*).

The contribution of positive charge and an RNA-like sugar conformation have been combined in the 2′-*O*-(2-aminoethyl) (AE) ribose derivatives developed by Cuenoud and colleagues (*39*−*41*). TFOs carrying these substitutions show enhanced kinetics of triplex formation and greater stability of the resultant complex at physiological pH and low Mg^{2+} concentration. NMR analysis indicates that the CH_2-CH_2 in the 2′-AE side chain is exclusively in the *gauche*$^+$ conformation, resulting in a specific interaction between the amine and the i-1 phosphate group in the purine strand of the duplex (*42*).

We are developing TFOs as gene-targeting reagents for use in mammalian, including human, cells. We assess bioactivity in a gene knockout assay, which measures the frequency of hypoxanthine phosphoribosyltransferase (*HPRT*) gene-deficient cells following treatment with a TFO, linked to psoralen, designed to target a site in the gene. In earlier work we showed that in *HPRT*-deficient clones the mutations were localized to the target region (*16*). Recently we described TFOs containing extensive 2′-AE residues, again linked to the psoralen, that were active in the *HPRT* knockout assay (*43*). It was noteworthy that the most highly substituted oligonucleotides, although active in biochemical assays, were the least effective in the biological assay. These results indicated that the bioassay is sensitive to features of the oligonucleotides that are not reported by the biochemical measurements. Thus, it seems that the design of bioactive 2′-AE TFOs must reflect the need for sufficient 2′-AE content to enable function in a physiological environment, while avoiding the apparently disabling effects of too much substitution. Here we have characterized TFOs with relatively modest levels of 2′-AE residues and identified the substitution format that shows robust bioactivity as monitored in the *HPRT* assay.

EXPERIMENTAL PROCEDURES

*Synthesis of 2′-AE-5-methyluridine Controlled Pore Glass (CPG) (Scheme 1). 5′-O-(4,4′-Dimethoxytrityl)-5-methyluridine-2′-O-(2-aminoethyl) 3′-O-Succinate (44), **2***. 5′-*O*-(4,4′-Dimethoxytrityl)-5-methyluridine-2′-*O*-(2-aminoethyl) (**1**, 0.45 g, 0.643 mmol) was dissolved in anhydrous dichloromethane (5 mL), and 0.128 g (1.28 mmol) of succinic anhydride was added to the solution. Subsequently, 78.1 mg (0.64 mmol) of 4-(dimethylamino)pyridine (DMAP) was added, and the mixture was stirred for 90 min. After completion of the reaction (as indicated by TLC), the solvent was evaporated in vacuo. The residual yellow oil was dissolved in dichloromethane and washed twice with 10% $NaHCO_3$(aq). The extracted organic phase was dried over Na_2SO_4 and evaporated in vacuo to yield a white solid, **2** (0.43 g, 85%): MS (HR-FAB), *m*/*z* 821.726 $(M + Na)^+$.

*5′-O-(4,4′-Dimethoxytrityl)-5-methyluridine-2′-O-methyl-3′-O-succinamido-N⁶-hexanamido-N³-propyl CPG, **3***. The 3′-succinate block (**2**) (128 mg, 0.16 mmol) was coevaporated with anhydrous pyridine and then dissolved in anhydrous DMF (2 mL). Subsequently, 85 μL (0.5 mmol) of *N*,*N*-diisopropylethylamine (DIEA) was added. A solution of 76 mg (0.2 mmol) of HATU in DMF was added to the mixture with stirring. Stirring was continued for ∼1 min to allow preactivation before the mixture was added to 1.25 g of acid-treated LCAA CPG (initial loading = 90 μmol/g), and the suspension was shaken for 16 h. Subsequently, the resin was washed with DMF, DCM, and CH_3CN. The unreacted amino groups of the resin were capped by shaking the resin with 0.36 mL (3 mmol) of ethyl trifluoroacetate and 0.42 mL (3 mmol) of TEA in 6 mL of MeOH. Finally, the resin was washed with MeOH, CH_3CN, and DCM and dried in vacuo. The loading on the CPG was determined by DMT release assay (final loading = 30 μmol/g).

Scheme 1[a]

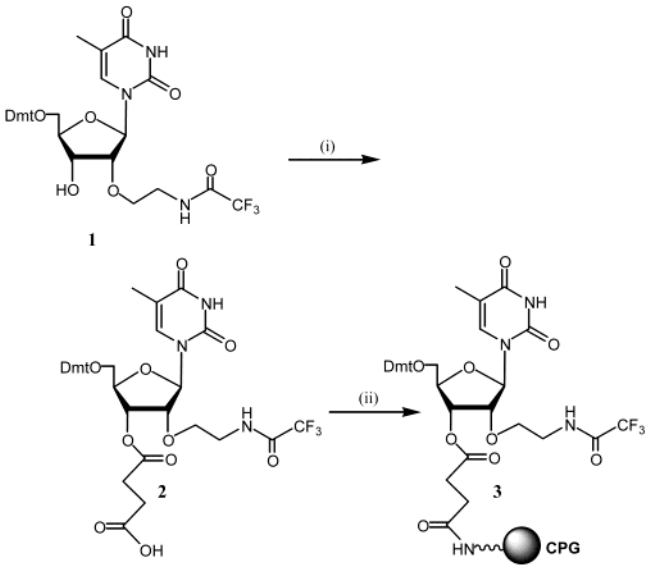

[a] (i) Nucleoside **1**, succinic anhydride (2 equiv), DMAP [4-(dimethylamino)pyridine, 1 equiv], CH_2Cl_2, RT, 1 h; (ii) LCAA-CPG (long-chain alkylamine controlled pore glass, initial loading = 90 mol/g), succinate **2** (1.5 equiv), HATU [O-(7-azabenzotriazol-1-yl)-1,1,3,3-tetramethyluronium hexafluorophosphate, 2 equiv], DIEA (*N*,*N*-diisopropylethylamine, 5 equiv), DMF, RT, 16 h; final loading as determined by DMT-assay = **3**, 30 mol/g.

Synthesis of TFOs. 5′-*O*-(4,4′-Dimethoxytrityl)-5-methyluridine-2′-*O*-methyl-3′-*O*-(β-cyanoethyl-*N*,*N*-diisopropyl)-phosphoramidite, *N*⁴-formamidine-5′-*O*-(4,4′-dimethoxytrityl)-5-methylcytidine-2′-*O*-methyl-3′-*O*-(β-cyanoethyl-*N*,*N*-diisopropyl)phosphoramidite, 5′-*O*-(4,4′-dimethoxytrityl)-5-methyluridine-2′-*O*-methyl-3′-*O*-succinamido-*N*⁶-hexanamido-*N*³-propyl CPG support, and 6-[4′-(hydroxymethyl)-4,5′,8-trimethylpsoralen]hexyl-1-*O*-(β-cyanoethyl-*N*,*N*-diisopropyl)phosphoramidite were purchased from Chemgenes, Ashland, MA. For the synthesis of 5′-*O*-(4,4′-dimethoxytrityl)-5-methyluridine-2′-*O*-(2-aminoethyl)-3′-*O*-(β-cyanoethyl-*N*,*N*-diisopropyl)phosphoramidite and *N*⁴-(*N*-methylpyrrolidineamidine)-5′-*O*-(4,4′-dimethoxytrityl)-5-methylcytidine-2′-*O*-(2-aminoethyl)-3′-*O*-(β-cyanoethyl-*N*,*N*-diisopropyl)phosphoramidite previously reported procedures were followed (*39*, *40*, *45*). The oligonucleotides were synthesized on CPG supports (500 Å) using an Expedite 8909 synthesizer using previously described procedures (*43*).

Deprotection and Purification of TFOs. The CPG support with a pso-TFO was placed in a vial closed with a porous

filter cap for gas-phase deprotection (*43*). The vial was inserted in an enclosed steel pressure chamber with a valve and evacuated by house vacuum. The valve was then connected to the gas cylinder, keeping the steel chamber under reduced pressure. The chamber was incubated with anhydrous methylamine gas (Aldrich) at room temperature for 45 min, followed by the release of the methylamine gas. The TFO was then taken up in distilled water. Analytical and semipreparative anion exchange (IE)-HPLC was carried out using a Dionex DNAPac PA-100 column (4.0 × 250 mm and 9.0 × 250 mm, respectively) on a Shimadzu HPLC system (LC-10ADvp) with a dual wavelength detector (SPD-10AVvp) and an autoinjector (SIL-10ADvp). The column was eluted using linear gradients of sodium chloride (0−1.0 M) in 0.1 M Tris buffer (pH 7.0) at a flow rate of 1.0 mL/min and monitored at wavelengths of 254 and 315 nm (λ_{max} for psoralen). The purified oligos were characterized by capillary zone electrophoresis and matrix-assisted laser desorption time of flight.

Thermal Denaturation Experiments. The TFO and the constituent strands of the target duplexes (5′ TCAGAAGA-AAAAAGAGAAA; 5′ TTTCTCTTTTTTCTTCTGA) were taken in buffers A−D [50 mM Tris, 100 mM NaCl, and 2 mM $MgCl_2$ (pH 6.0, 6.5, 7.0, and 7.5 respectively)]. These solutions were heated at 80 °C for 3 min and allowed to come to room temperature in 30 min. The TFO/duplex target solutions were incubated at 4 °C overnight. The thermal denaturation experiments were carried out in buffers A−D using a Cary 3E UV−visible spectrophotometer fitted with a thermostat sample holder and temperature controller. Triplexes were heated from 10 to 85 °C at a rate of 0.4 °C/min, and the absorbance at 260 nm was recorded as a function of the temperature. The data were processed using SigmaPlot 5.0 software to determine the first derivative of the melting curves and the T_m value was obtained. Each analysis was done two times, and the error was no more than 0.5 °C.

K_d Determination. A snapback duplex oligonucleotide containing the Chinese hamster intron 4/exon 5 HPRT target sequence (5′ AGTAGAAGAAAAAAGAGAAATGATTT-TCATTTCTCTTTTTTCTTCTACT) was synthesized and labeled by incubation with T4 DNA kinase and ^{32}P ATP. The radioactive oligonucleotide at a final concentration of 100 pM was incubated with various concentrations of the TFOs in buffer consisting of 20 mM Hepes, pH 7.2, and 10 or 1 mM $MgCl_2$ as indicated, at room temperature for 24 h. Samples were then loaded on a 15% acrylamide gel in Hepes buffer, pH 7.2, containing the appropriate level of $MgCl_2$ and electrophoresed for 16 h. The relative intensity of the duplex and triplex bands was determined by Phosphorimager analysis. The K_d values were determined by Hill's equation [$y = ax^b/(c^b + x^b)$], where y = percent triplex formation, x = TFO concentration, a = maximum percent value of triplex formation, b = Hill's coefficient (see legend of Figure 5b,c), c = approximate value of K_d. The assumptions on the basis of which the Hill's equation was used are (1) TFOs do not interact with themselves and (2) the concentration of the duplex target is too small to influence the equilibrium of triplex formation. The data were processed with SigmaPlot 5.0 software.

In Vivo Stability. Details of this procedure have been described previously (*46*). The method measures the stability of a preformed triplex following introduction of the complex into cells. The psupF12 shuttle vector plasmid was engineered to contain the CHO HPRT triplex binding site in the pre-tRNA portion of a variant supF mutation reporter gene, immediately adjacent to the mature gene sequence (see ref *43* for the schematic of the supF12 gene). The first two bases of the mature gene sequence were 5′ TA, which is a sequence appropriate for psoralen cross-linking. A psoralen-linked TFO, by forming a triplex with the target sequence, positions the psoralen at the TA step such that a cross-link is introduced upon photoactivation. Replication and/or repair of the cross-link in mammalian cells will introduce mutations at the site, and these can be quantitated in a microbiological screen of the supF gene in the progeny plasmids, following recovery from the mammalian cells. A cross-link is required for mutagenesis, photoactivation is required for cross-linking, and the positioning of the psoralen is dependent on an intact triplex. Thus, the mutation frequency is a reflection of the triplexes present in the plasmid population at the time of photoactivation. Triplexes were formed by incubation of a TFO and the psupF12 plasmid (20 mM Hepes, pH 7.2, 10 mM $MgCl_2$, 2 μM TFO, 0.6 pmol of plasmid), unbound TFO was removed, and the plasmid−TFO complexes were electroporated into Cos-1 cells. At various times after transfection the cells were exposed to long-wave ultraviolet light (365 nm, 3 min, 1.8 J/cm^2, in a Rayonet chamber). The cells were incubated for an additional 48 h, during which time the psoralen cross-links were repaired, some with mutational consequences, and the plasmid was replicated. Progeny plasmids were then harvested, treated with *Dpn*I to remove nonreplicated input plasmids (*47*), and introduced into the *Escherichia coli* indicator strain MBM 7070 (*48*). The bacteria were spread on plates containing isopropyl 1-thio-β-D-galactopyranoside and 5-bromo-4-chloro-3-indolyl β-D-galactopyranoside, and the frequency of white or light blue colonies, which contained plasmids with mutations in the supF gene, was determined.

HPRT Knockout Assay. Chinese hamster ovary (CHO) cells were grown in Dulbecco's modified Eagle medium (DMEM) supplemented with penicillin, streptomycin, glutamine, and 10% fetal calf serum. Cells were cultured in HAT medium (10^{-4} M hypoxanthine, 5×10^{-6} M aminopterin, and 10^{-5} M thymidine) for 1 week to remove pre-existing *HPRT*-deficient cells. They were treated as described previously (*49*), a procedure that enhances knockout activity and will be described in a future publication. The TFOs were introduced by electroporation (Bio-Rad, 130 V, 960 μF) with 3×10^6 cells suspended in 200 μL with each TFO at 5 μM. They were incubated at room temperature for 3 h and exposed in a Rayonet chamber to UVA light for 3 min at 1.8 J/cm^2. The cells were plated in complete medium for 8−10 days with two to three passages and then placed in selective medium depleted of hypoxanthine and containing 20 μM thioguanine (200,000 cells/100-mm dish). Cells were also plated in selective medium without thioguanine to determine plating efficiency. After 10 days, resistant colonies were counted and picked for expansion and DNA analysis.

A similar protocol was observed when the frequency of cells with mutations in adenosine phosphoribosyltransferase (*APRT*) was determined. CHO-AT3 (hemizygous for *APRT*) cultures were cleared of *APRT*-deficient cells by growth in 10 μM azaserine and 20 μM adenine. Selections for *APRT*-

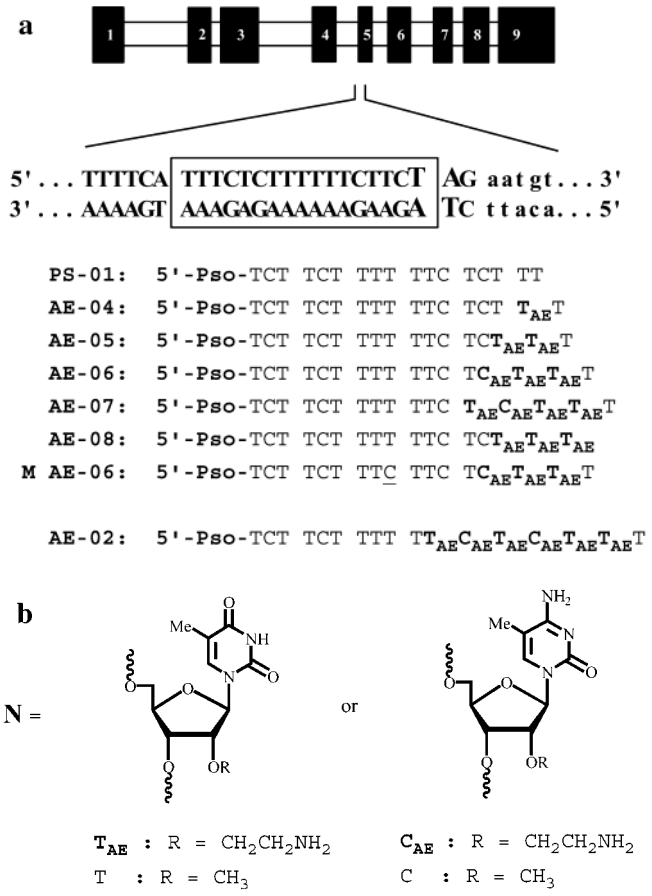

FIGURE 1: (a) Sequence of the *HPRT* I4/E5 target and the TFOs with various patterns of 2′-AE substitution. The target is in intron 4 adjacent to exon 5 (shown in small letters). The TA step displaying the psoralen cross-link site is shown in bold. The TFOs are parallel to the purine strand in the triplex. M AE-06 has a single mismatch (the underlined C). (b) Structures of 2′-substituted (2′-OMe and 2′-AE), 5-methylcytidine (C) and 5-methyluridine (T).

deficient colonies were done in medium containing 50 μg/mL aza-adenine.

RESULTS

The target sequence and location in the Chinese hamster *HPRT* gene are shown in Figure 1a. Also indicated are the sequences and substitution patterns of the oligonucleotides described in this paper. Each oligonucleotide contained 5-methylcytosine, and all sugar residues were either 2′-OMe or 2′-AE (Figure 1b). All oligonucleotides were linked to psoralen as described previously (*43*). In contrast to our earlier study in which we characterized oligonucleotides with extensive 2′-AE substitution, including AE-02 (Figure 1a) (*43*), in the experiments described here we have defined the minimum number of 2′-AE residues required for gene knockout activity in vivo.

Thermal Stability of Triplexes Formed by 2′-AE TFOs. Triplexes were formed by incubation of individual TFOs with a 19-mer duplex oligonucleotide (Experimental Procedures) containing the I4/E5 CHO *HPRT* target sequence in buffers ranging from pH 6.0 to 7.5. Gel shift analysis demonstrated the formation of triplexes by each TFO (not shown). We then measured the thermal stability of the triplexes in each buffer (Experimental Procedures). The analysis, in pH 7.0 buffer, of the triplex formed by the duplex and a third strand

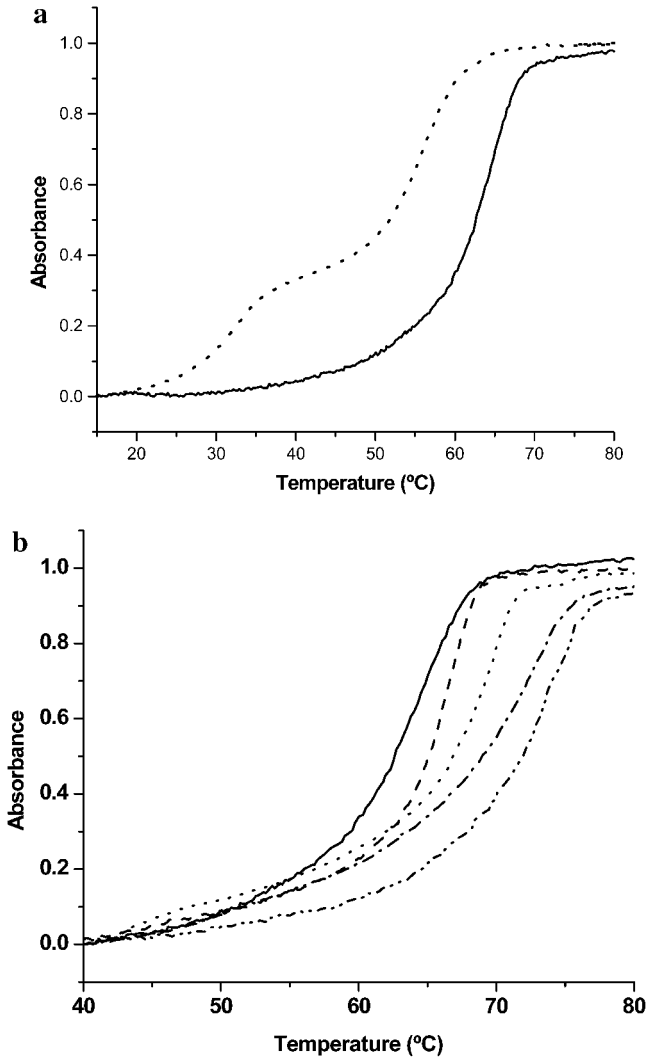

FIGURE 2: (a) Absorbance at 254 nm versus temperature showing triplex and duplex melts of the deoxynucleotide analogue of PS-01 (dot) and Ps-01 (solid) with the 19-mer duplex. A two-step transition [first transition, Hoogsteen base pair (bp) melt; second transition, Watson−Crick bp melt] is observed for the deoxynucleotide analogue of PS-01 (dot), whereas a one-step change (single transition, combined Hoogsteen bp and Watson−Crick bp melt) is seen for PS-01 (solid). (b) Absorbance at 254 nm versus temperature showing the increments in the single-transition melts of the complexes of PS-01 (solid), AE-04 (dash), AE-05 (dot), AE-06 (dash dot), and AE-07 (dash dot dot) with the 19-mer duplex target (Experimental Procedures).

containing deoxyribose sugars showed two transitions with the triplex T_m (31.3 °C) below the duplex T_m (55.1 °C) (Figure 2a). In contrast, the triplex formed by the TFO containing all 2′-OMe sugars (PS-01) showed a single transition with a T_m (63.8 °C) higher than the duplex T_m (see supplementary table). This result demonstrated that the presence of the 2′-OMe ribose in the third strand had a profound effect on triplex stability. The profiles, at pH 7.0, of the triplexes formed by the TFOs containing 2′-AE residues are shown in Figure 2b. As expected, there was a progressive increase in T_m (∼2.0 °C/2′-AE residue) as the 2′-AE content increased (*39*), and there was a single transition with each triplex. For the sake of economy the TFOs examined in the thermal melting study were those used in the biological experiments. Because they were linked to psoralen, we were concerned that possible photoactivation

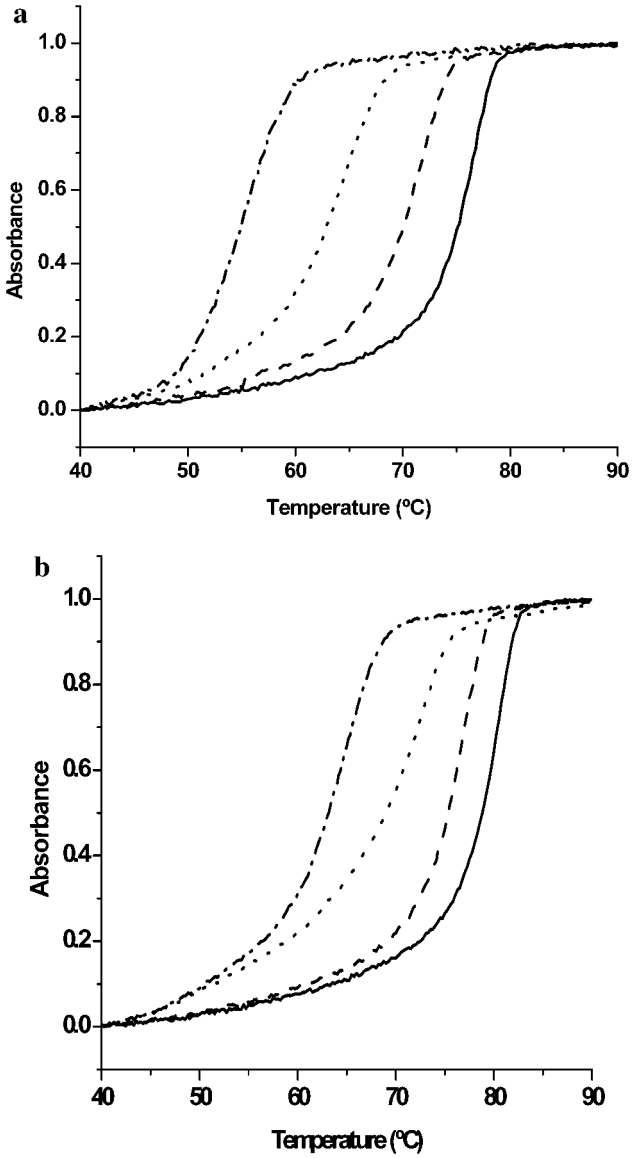

FIGURE 3: (a) Melting curve of triplexes of Ps-01 with 19-mer duplex at pH 6.0 (solid), pH 6.5 (dash), pH 7.0 (dot), and pH 7.5 (dash dot). (b) Melting curve of triplexes of AE-06 with 19-mer duplex target (Experimental Procedures) at pH 6.0 (solid), pH 6.5 (dash), pH 7.0 (dot), and pH 7.5 (dash dot).

of the psoralen in the spectrophotometer would compromise interpretation of the results. However, control experiments showed that TFOs without psoralen displayed the same melting profiles, whereas deliberate photoactivation of the psoralen after triplex formation resulted in profiles with transitions 15 °C above those shown here. Consequently, we concluded that the psoralen was not photoactivated in the cuvette and the presence of the psoralen had no effect on the T_m values.

A hallmark of pyrimidine motif triplexes is their sensitivity to increase in pH. Analysis of the triplexes formed by the PS-01 TFO as a function of pH (from 6 to 7.5) showed the predictable decline in T_m as the pH was increased (Figure 3a). (In control experiments the T_m of the duplex was indifferent to pH.) In all curves there was a single species, and only at the highest pH was this single transition coincident with that of the duplex shown in Figure 2a. The same analysis with the triplex formed by the TFO with three 2′-AE substitutions showed a less pronounced decline in T_m

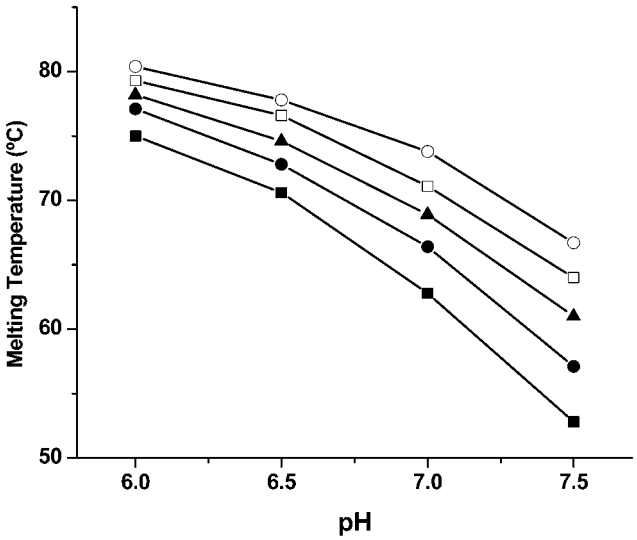

FIGURE 4: Graphic representation of drop in T_m as a function of pH, from pH 6.0 to pH 7.5, for PS-01 (solid square), AE-04 (solid circle), AE-05 (triangle), AE-06 (open square), and AE-07 (open circle).

as the pH rose, with the T_m at pH 7.5 being greater than that of the duplex (Figure 3b). An analysis of T_m versus pH for the triplexes formed by all the TFOs demonstrated that the T_m differential (low to high pH) narrowed as the 2′-AE content increased (Figure 4). When the pH was increased from 6.0 to 7.5, the decline in T_m was 15.2 °C for AE-06 and 14.2 °C for AE-07, whereas for PS-01 it was 20.7 °C. Thus, the presence of the 2′-AE residues partially ameliorated the destabilizing effects of pH in the physiological range.

Aminoethoxy Residues Enhance TFO Affinity. We measured the K_d of the TFOs in gel shift assays (Experimental Procedures). The determinations were made in buffers at pH 7.2 containing either 10 or 1 mM $MgCl_2$. The latter condition was of particular interest because the level of free Mg^{2+} in cells is believed to be much lower than 10 mM. The binding isotherms for PS-01 and AE-06 in 1 mM $MgCl_2$ are shown in Figure 5a. AE-06 had a lower K_d (148 nM) than PS-01 (376 nM). The values of K_d for each of the TFOs at 10 and 1 mM $MgCl_2$ are shown in Figure 5b,c. The presence of 2′-AE residues resulted in a decrease in K_d (relative to PS-01) at both $MgCl_2$ concentrations, although this was more pronounced in 1 mM $MgCl_2$. Interestingly, in the lower concentration of $MgCl_2$, the K_d values of AE-06 and AE-07 were lower than would have been expected from the simple proportionality predicted by the results with the TFOs with zero, one, or two 2′-AE residues. The assay was also performed in 1 mM $MgCl_2$ with M AE-06, which had the same three adjacent 2′-AE residues as in AE-06 but a single change in sequence (a C instead of T in the middle of the oligonucleotide). The affinity of this TFO was very poor, and half-maximal binding was not observed at 4 μM, the highest concentration used in the assay (not shown).

Triplexes Formed by TFO AE-06 Are More Stable in Vivo. We have developed a method for measuring the stability of triplexes, preformed in vitro, in the cellular compartment that supports replication and mutagenesis (*46*). The assay is based on a shuttle vector plasmid carrying a variant supF gene that serves as a mutation marker and containing the CHO *HPRT* triplex target embedded in the gene. Preformed triplexes on the plasmid were electroporated into mammalian cells and,

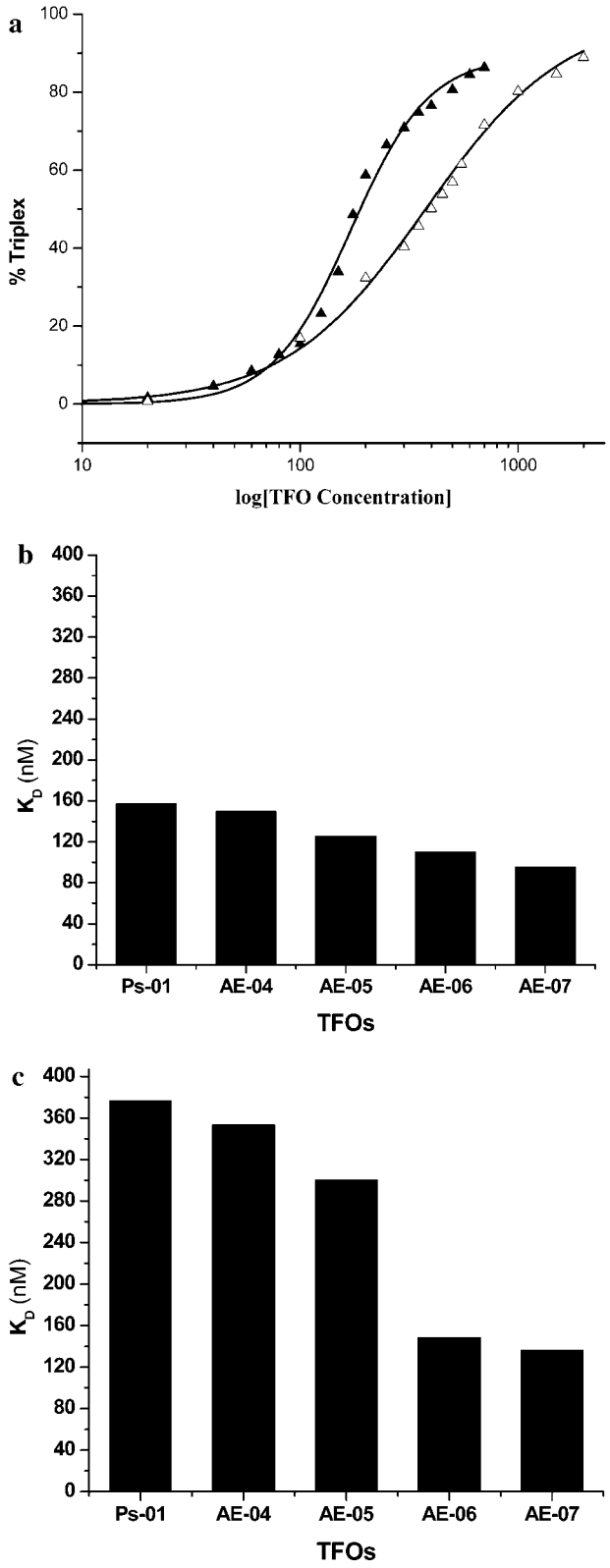

FIGURE 5: (a) Binding isotherms of PS-01 (open triangles) and AE-06 (solid triangles) in 1 mM $MgCl_2$. (b) TFO K_d at 10 mM $MgCl_2$. Hill's coefficients: Ps-01, 0.95; AE-04, 1.63; AE-05, 1.53; AE-06, 1.82; AE-07, 1.01. (c) TFO K_D at 1 mM $MgCl_2$. Hill's coefficients: Ps-01, 1.35; AE-04, 1.84; AE-05, 1.37; AE-06, 2.43; AE-07, 1.97. The values of K_d are in the nanomolar scale.

as a function of time after introduction, the cells were exposed to UVA light to trigger psoralen cross-linking of the plasmids containing triplexes. Plasmids that lost the triplex would not be cross-linked and would not incur

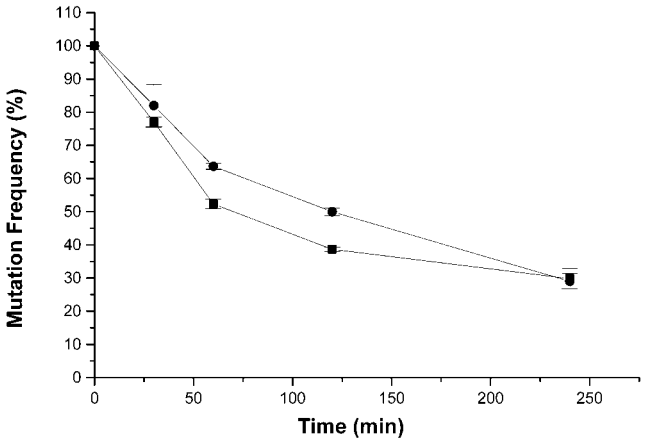

FIGURE 6: Stability of preformed triplexes in the cellular replication and mutagenesis compartment. Triplexes were preformed on psupF12 with PS-01 (squares) and AE-06 (circles) and introduced into Cos 1 cells by electroporation. At the indicated times the cells were exposed to UVA light to photoactivate the psoralen. After an additional 48 h, the replicated plasmids were harvested and screened for mutations in the supF12 gene in a microbiological screen. Three independent experiments were performed with each TFO, and the data points represent the mean and the standard error of the mean.

mutations. We compared the stability of triplexes formed by PS-01 and AE-06. As shown in Figure 6 the triplex formed by AE-06 ($t_{1/2}$ = 120 min) was twice as stable in the cells as the PS-01 triplex ($t_{1/2}$ = 59 min). These data indicated that the triplex formed by the TFO with three AE residues was more resistant to the cellular environment than the PS-01 triplex. Interestingly, the AE-06 triplex was more stable than those formed by the TFOs with more extensive 2′-AE substitution (for example, AE-02, with six residues), described in our earlier study (*43*).

Activity of 2′-AE TFOs in the HPRT Knockout Assay. The pso-TFOs were introduced into CHO cells by electroporation (Experimental Procedures). After 3 h, the cells were exposed to UVA, cultured for 8−10 days, and then plated in medium containing 6-thioguanine (6-TG). Resistant colonies were counted, and the results are shown in Figure 7a. Cells treated with the TFO containing only 2′-OMe sugars, or with the TFO with a single 2′-AE substitution, showed few 6-TG resistant colonies relative to mock electroporated control cultures. A fewfold more colonies were recovered when the TFO with two substitutions was tested. In contrast, there was a substantial increase in activity with AE-06 and AE-07, with the frequency of TG-resistant colonies slightly more than 0.1 and 0.14%, respectively, ~300−400-fold over the background. It should be noted that the background mutation frequency reflects the occurrence of inactivating spontaneous mutations across the entire coding region of the *HPRT* gene, quite different from the localization of events targeted by the TFO. As in our previous work, UVA treatment was required for a signal, indicating that psoralen activation was critical for mutagenesis. A single, central, base change in the TFO sequence abolished activity (M AE-06).

To test for possible activity of the TFOs against unintended targets, the experiment was repeated with the cells exposed to selection for mutations in the *APRT* gene. However, we recovered *APRT*-deficient cells at frequencies little different from background levels (Figure 7b). These results argued that the TFO targeting was specific to the intended *HPRT* target, at least as monitored at the level of another gene.

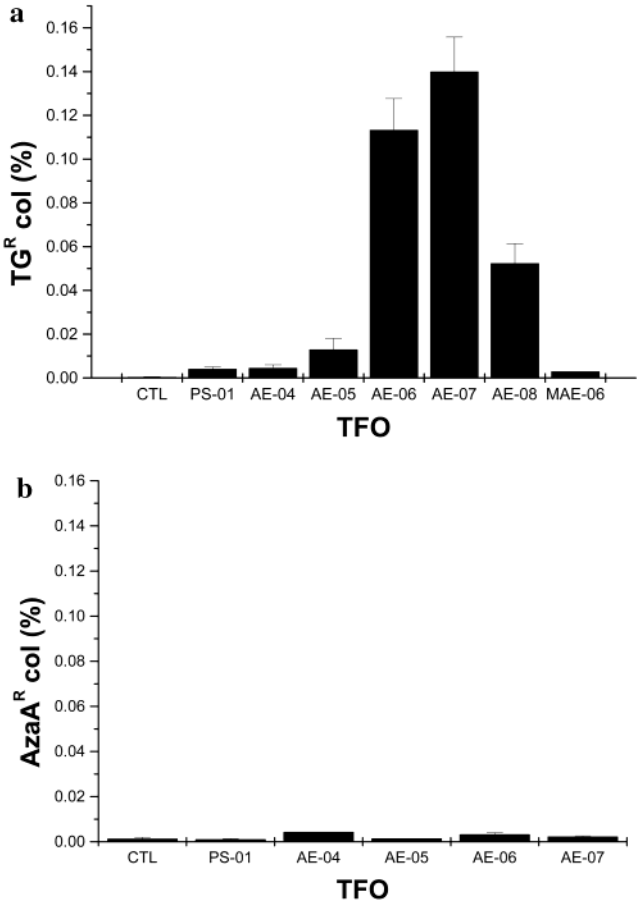

FIGURE 7: (a) Frequency of *HPRT*-deficient cells following treatment with pso-TFOs. TFOs were electroporated into CHO cells and the cells treated with UVA 3 h later. The cells were carried for 8−10 days and then placed in thioguanine selection medium; companion cultures were placed in nonselective medium to score plating efficiency. Results are expressed as the percent of cells that were thioguanine resistant, corrected for plating efficiency. Mean and standard errors of the mean: PS-01, 0.004 ± 0.0008; AE-04, 0.005 ± 0.001; AE-05, 0.01 ± 0.005; AE-06, 0.11 ± 0.01; AE-07, 0.14 ± 0.04; AE-08, 0.05 ± 0.01. Results for AE-06 represent nine independent determinations, whereas seven independent experiments were performed with AE-07 and AE-08. (b) Activity of the TFOs in CHO cells against the *APRT* gene. Cells were placed in azaadenine to select for cells deficient in *APRT*.

This was further supported by analysis of the mutations in TG^R clones, which showed the same events reported previously—principally small deletions, all in the target region (not shown, but see ref *43*).

2′-AE-cytosine versus 2′-AE-thymidine. AE-06 contains three 2′-AE-substituted nucleotides, two thymidines and one cytosine. Cytosines may be at least partially protonated when in pyrimidine motif triplexes, even under physiological conditions (*18*). It was of interest to measure the activity of a TFO containing three adjacent AE-thymidines in which the only positive charge in the 2′-AE patch would be contributed by the sugar modification. Accordingly, we prepared AE-08, containing three 2′-AE-thymidines at the 3′ terminus of the oligonucleotide. This required synthesis of the 2′-AE-thymidine CPG support as described under Experimental Procedures. The K_d of this TFO (160 nM, 1 mM Mg^{2+}) and the thermal stability of the AE-08 triplex (70.3 °C, pH 7.0) were similar to the data with AE-06. However, this TFO quite reproducibly showed ~50% of the activity of AE-06 in the HPRT assay (Figure 7a), indicating that the 2′-AE-cytosine offered a measurable enhancement to the bioactivity of the TFO. Thus, the bioassay could distinguish between the two TFOs, whereas our biochemical measurements did not. This may be the result of the environment in which triplex formation occurs (ionic composition, local pH, etc.) or a reflection of enzymatic functions that stabilize or destabilize triplexes or those that convert the targeted cross-link into a mutation.

DISCUSSION

The utilization of TFOs for genomic manipulation will require the development of oligonucleotides that can form stable triplexes in the context of the nuclear environment. Base and sugar modifications have the potential to overcome the classical limitations imposed by physiological pH and Mg^{2+} concentration. In the experiments described here our concern has been to identify an oligonucleotide modification format that supports reproducible bioactivity. We have taken as a point of departure pyrimidine TFOs uniformly substituted with 2′-OMe ribose. This modification imparts a C3′-*endo* conformation to the sugar and preorganizes the single-strand TFO into a conformation similar to that in the triplex (*50*). This has the salutary effect of reducing some of the entropic barriers to triplex formation (*51*), a concept that has stimulated the synthesis of TFOs with other "preorganizing" sugar modifications (*39*, *52*) (see ref *53* for a discussion of the limits to this strategy). However, it is clear from our previous results (*16*, *43*), and those presented here, that although the 2′-OMe substitution improves triplex stability, it is insufficient for biological activity. The 2′-AE modification maintains the C3′-*endo* conformation and also adds a positive charge. This reduces the negative charge repulsion between the third strand and the duplex prior to triplex formation and stabilizes the triplex after formation through an interaction between the amine and the i-1 phosphate of the duplex target (*39*). In our previous study (*43*) we examined TFOs with extensive 2′-AE substitution and found that they showed only moderate biological activity. In this paper we show, in contrast, that a rather modest level of substitution results in significant bioactivity as monitored by the *HPRT* knockout assay.

Triplex Stability. The thermal stability experiments revealed two interesting features of the triplexes formed by the TFOs. The first is that the replacement in the third strand of deoxyribose with 2′-OMe ribose resulted in single transition melting curves with T_m values of the triplexes higher than the T_m of the duplex target. Triplexes formed by pyrimidine oligonucleotides with 2′-hydroxyl (*26*) or 2′-OMe ribose (*28*) yield single transition melting profiles, with, under some conditions, T_m values greater than the duplex targets (*28*, *54*). There have also been reports of quite stable purine motif triplexes (*55*, *56*). The high T_m is due to an increase in the stability of the interaction of the third strand and the purine strand of the duplex. Disruption of the third-strand interaction is followed immediately by melting of the duplex, and only a single transition is observed. It has been argued that third strands containing 2′-OMe sugars impose a lower degree of distortion on the underlying duplex than third strands containing deoxyribose and that there are van der Waals interactions between the methyl groups and the i-1 purine residue in the duplex. These factors can explain the greater stability of these triplexes (*50*). The 2′-AE

modifications, by maintaining the preorganization of the third strand and introducing a positive charge, further strengthen the interaction between the third strand and the purine strand of the duplex (*39*).

The second noteworthy observation is that the triplexes formed by TFOs with 2′-AE residues were more resistant to increase in pH as compared to the PS-01 triplex. The decline in stability of triplexes in the pyrimidine motif as the pH is increased is ascribed to the loss of cytosine protonation (*3*, *7*, *57*). Although the consequent elimination of a hydrogen bond has often been taken as the basis for the decline in triplex stability, it has been shown that the loss of the positive charge is the more critical factor (*18*). Because the pK_a of the amino group on the 2′-AE is 8.5−9.0, it would be protonated at physiological pH. Apparently the positively charged 2′-AE sugars partially compensate for loss of cytosine charge as the pH moves to the physiological range.

Three and Four 2′-AE Residues Disproportionately Enhance TFO Affinity and Bioactivity. The importance of the positive charge contributed by the AE substitution permits triplex formation in buffers containing relatively low levels of Mg^{2+}, as has been emphasized in earlier publications on TFOs with AE substitutions (*39*, *40*). In our determination of TFO K_d we observed relatively little difference between the oligonucleotides when the assays were performed in 10 mM Mg^{2+}. The differences were more apparent when the assays were done in 1 mM Mg^{2+}. The most interesting feature of those measurements was the drop in K_d, sharper than expected, as the AE content went from two to three or four. These results hinted that the AE-06 and -07 TFOs might differ from AE-05 more than expected from the simple addition of an 2′-AE residue.

The difference between the TFOs was more pronounced in the *HPRT* knockout assay. AE-06 was 10-fold, and AE-07 14-fold, more active than AE-05. These results were confirmed in many experiments with independent preparations of the TFOs, with different cell culture stocks. Consequently, we have concluded that, minimally, three 2′-AE substitutions are sufficient to confer bioactivity on these TFOs.

What facet of TFO activity could be the basis of the discontinuity in bioactivity between the oligonucleotide with two 2′-AE residues and those with three or four? Triplex formation proceeds through a nucleation−elongation process (*51*, *58*, *59*) with the nucleus consisting of three to five base triplets (*58*, *60*). Following nucleation, triplex formation either fails due to third-strand dissociation or is completed by a zipper mechanism, similar to that described for duplex formation (*61*). The activity of a TFO in triplex formation reflects the probability of nucleation, the stability of the nucleus, the rate of elongation, and also the persistence of the complete structure once formed.

In the experiments presented here we have described two measures of the stability of preformed triplexes, one biophysical and one biological. The thermal melting analysis, performed at physiological pH, indicated that the distinction between TFOs was incremental and essentially proportional to the 2′-AE content. The biological assay, which measures the stability of preformed triplexes in the cellular replication compartment (*46*), reported only a 2-fold difference in triplex half-life between AE-06 and PS-01 (a TFO with lower biological activity than AE-05). Although these are not exhaustive studies, we think it unlikely that the sharp difference in *HPRT* knockout activity between AE-05 and AE-06/AE-07 represents pronounced differences in the persistence of triplexes formed by these TFOs with the chromosomal target in vivo. Instead, it seems more probable that the TFOs are distinguished by their activity during the nucleation and/or elongation phases of triplex formation. This is consistent with the conclusions of the initial description of 2′-AE TFOs—that the contacts between the AE side chains and the phosphate backbone of the duplex make an important contribution to the rate of association of the third strand with the duplex (*39*). Three and four 2′-AE residues may support the formation of a more stable nucleus in vivo than do two residues, with a corresponding greater probability of successful elongation. Of course, a clear understanding of the basis for the difference between TFOs with two or three substitutions will require additional study.

Whereas the distinction between AE-05 and AE-06 may have a straightforward biophysical basis, our observation that more extensive 2′-AE substitution is counterproductive in the bioassay is not as readily explained. The AE-02 TFO (with six AE residues), from our previous study, formed quite stable triplexes (T_m = 76.8 °C, pH 7.0), but was only one-fourth to one-fifth as active as AE-06 and AE-07 (*43*). We have observed that the greater AE content in the earlier TFOs, although it improves biochemical parameters such as T_m and K_d, increases adherence to surfaces (the oligonucleotides become more sticky), and this may reduce the effective intracellular concentration and, thus, the bioactivity (*43*). Whatever the explanation, the result emphasizes the need for informative bioassays as a guide to TFO development and underscores our incomplete understanding of the relationship between the in vitro and in vivo activities of a TFO.

The most important conclusion from the data presented here is that the TFOs with three or four 2′-AE residues (preferably including a 2′-AE-cytosine) are reliably bioactive at levels that permit experimentation on a variety of important issues. These include questions regarding the influence of the biology and physiology of the cell on TFO activity and the influence of different DNA repair functions on the efficiency of gene knockout. These TFOs can serve as references for the next generation of oligonucleotides with other, or additional, chemical modifications. It should be possible to measure the bioactivity of these TFOs linked to different DNA reactive compounds. Finally, we expect that this format will also be useful in developing TFOs containing base analogues that successfully expand target sequence options (*62*−*64*).

SUPPORTING INFORMATION AVAILABLE

Table of triplex melting temperatures. This material is available free of charge via the Internet at http://pubs.acs.org.

REFERENCES

1. Felsenfeld, G., Davies, D. R., and Rich, A. (1957) *J. Am. Chem. Soc. 79*, 2023−2024.
2. Moser, H. E., and Dervan, P. B. (1987) *Science 238*, 645−650.
3. Thuong, N. T., and Helene, C. (1993) *Angew. Chem., Int. Ed. Engl. 32*, 666−690.
4. Manor, H., Rao, B. S., and Martin, R. G. (1988) *J. Mol. Evol. 27*, 96−101.

5. Schroth, G. P., and Ho, P. S. (1995) *Nucleic Acids Res. 23*, 1977−1983.
6. Behe, M. J. (1995) *Nucleic Acids Res. 23*, 689−695.
7. Radhakrishnan, I., and Patel, D. J. (1994) *Biochemistry 33*, 11405−11416.
8. Frank-Kamenetskii, M. D., and Mirkin, S. M. (1995) *Annu. Rev. Biochem. 64*, 65−95.
9. Fossella, J. A., Kim, Y. J., Shih, H., Richards, E. G., and Fresco, J. R. (1993) *Nucleic Acids Res. 21*, 4511−4515.
10. Letai, A. G., Palladino, M. A., Fromm, E., Rizzo, V., and Fresco, J. R. (1988) *Biochemistry 27*, 9108−9112.
11. Helene, C., Thuong, N. T., and Harel-Bellan, A. (1992) *Ann. N. Y. Acad. Sci. 660*, 27−36.
12. Vasquez, K. M., and Wilson, J. H. (1998) *Trends Biochem. Sci. 23*, 4−9.
13. Maher, L. J., III (1996) *Cancer Invest. 14*, 66−82.
14. Neidle, S. (1997) *Anticancer Drug Des. 12*, 433−442.
15. Wang, G., Levy, D. D., Seidman, M. M., and Glazer, P. M. (1995) *Mol. Cell. Biol. 15*, 1759−1768.
16. Majumdar, A., Khorlin, A., Dyatkina, N., Lin, F. L., Powell, J., Liu, J., Fei, Z., Khripine, Y., Watanabe, K. A., George, J., Glazer, P. M., and Seidman, M. M. (1998) *Nat. Genet. 20*, 212−214.
17. Vasquez, K. M., Narayanan, L., and Glazer, P. M. (2000) *Science 290*, 530−533.
18. Asensio, J. L., Lane, A. N., Dhesi, J., Bergqvist, S., and Brown, T. (1998) *J. Mol. Biol. 275*, 811−822.
19. Blume, S. W., Lebowitz, J., Zacharias, W., Guarcello, V., Mayfield, C. A., Ebbinghaus, S. W., Bates, P., Jones, D. E., Jr., Trent, J., Vigneswaran, N., and Miller, D. M. (1999) *Nucleic Acids Res. 27*, 695−702.
20. Pesco, J., Salmon, J. M., Vigo, J., and Viallet, P. (2001) *Anal. Biochem. 290*, 221−231.
21. Lee, J. S., Woodsworth, M. L., Latimer, L. J., and Morgan, A. R. (1984) *Nucleic Acids Res. 12*, 6603−6614.
22. Povsic, T. J. a. P. B. D. (1989) *J. Am. Chem. Soc. 111*, 3059−3061.
23. Miller, P. S., Bi, G., Kipp, S. A., Fok, V., and DeLong, R. K. (1996) *Nucleic Acids Res. 24*, 730−736.
24. Lacroix, L., Lacoste, J., Reddoch, J. F., Mergny, J. L., Levy, D. D., Seidman, M. M., Matteucci, M. D., and Glazer, P. M. (1999) *Biochemistry 38*, 1893−1901.
25. Lacroix, L., Arimondo, P. B., Takasugi, M., Helene, C., and Mergny, J. L. (2000) *Biochem. Biophys. Res. Commun. 270*, 363−369.
26. Roberts, R. W., and Crothers, D. M. (1992) *Science 258*, 1463−1466.
27. Escude, C., Sun, J. S., Rougee, M., Garestier, T., and Helene, C. (1992) *C. R. Acad. Sci. III 315*, 521−525.
28. Shimizu, M., Konishi, A., Shimada, Y., Inoue, H., and Ohtsuka, E. (1992) *FEBS Lett. 302*, 155−158.
29. Torigoe, H., Hari, Y., Sekiguchi, M., Obika, S., and Imanishi, T. (2001) *J. Biol. Chem. 276*, 2354−2360.
30. Kukreti, S., Sun, J. S., Garestier, T., and Helene, C. (1997) *Nucleic Acids Res. 25*, 4264−4270.
31. Arya, D. P., and Bruice, T. C. (1999) *Proc. Natl. Acad. Sci. U.S.A. 96*, 4384−4389.
32. Escude, C., Giovannangeli, C., Sun, J. S., Lloyd, D. H., Chen, J. K., Gryaznov, S. M., Garestier, T., and Helene, C. (1996) *Proc. Natl. Acad. Sci. U.S.A. 93*, 4365−4369.
33. Dagle, J. M., and Weeks, D. L. (1996) *Nucleic Acids Res. 24*, 2143−2149.
34. Ehrenmann, F., Vasseur, J. J., and Debart, F. (2001) *Nucleosides Nucleotides Nucleic Acids 20*, 797−799.
35. Vasquez, K. M., Dagle, J. M., Weeks, D. L., and Glazer, P. M. (2001) *J. Biol. Chem. 276*, 38536−38541.
36. Bijapur, J., Keppler, M. D., Bergqvist, S., Brown, T., and Fox, K. R. (1999) *Nucleic Acids Res. 27*, 1802−1809.
37. Rajeev, K. G., Jadhav, V. R., and Ganesh, K. N. (1997) *Nucleic Acids Res. 25*, 4187−4193.
38. Sund, C., Puri, N., and Chattopadhyaya, J. (1996) *Tetrahedron 52*, 12275−12290.
39. Cuenoud, B., Casset, F., Husken, D., Natt, F., Wolf, R. M., Altmann, K. H., Martin, P., and Moser, H. E. (1998) *Angew. Chem., Int. Ed. Engl. 37*, 1288−1291.
40. Blommers, M. J., Natt, F., Jahnke, W., and Cuenoud, B. (1998) *Biochemistry 37*, 17714−17725.
41. Stutz, A. M., Hoeck, J., Natt, F., Cuenoud, B., and Woisetschlager, M. (2001) *J. Biol. Chem. 276*, 11759−11765.
42. Carlomagno, T., Blommers, M. J., Meiler, J., Cuenoud, B., and Griesinger, C. (2001) *J. Am. Chem. Soc. 123*, 7364−7370.
43. Puri, N., Majumdar, A., Cuenoud, B., Natt, F., Martin, P., Boyd, A., Miller, P. S., and Seidman, M. M. (2001) *J. Biol. Chem. 276*, 28991−28998.
44. Pon, R. T., Yu, S., and Sanghvi, Y. S. (1999) *Bioconjugate Chem. 10*, 1051−1057.
45. Manoharan, M., Prakash, T. P., Barber-Peoc'h, I., Bhat, B., Vasquez, G., Ross, B. S., and Cook, P. D. (2002) *J. Org. Chem. 64*, 6468−6472.
46. Lin, F. L., Majumdar, A., Klotz, L. C., Reszka, A. P., Neidle, S., and Seidman, M. M. (2000) *J. Biol. Chem. 275*, 39117−39124.
47. Peden, K. W., Pipas, J. M., Pearson-White, S., and Nathans, D. (1980) *Science 209*, 1392−1396.
48. Seidman, M. M., Dixon, K., Razzaque, A., Zagursky, R. J., and Berman, M. L. (1985) *Gene 38*, 233−237.
49. Orren, D. K., Petersen, L. N., and Bohr, V. A. (1995) *Mol. Cell. Biol. 15*, 3722−3730.
50. Asensio, J. L., Carr, R., Brown, T., and Lane, A. N. (1999) *J. Am. Chem. Soc. 121*, 11063−11070.
51. Kamiya, M., Torigoe, H., Shindo, H., and Sarai, A. (1996) *J. Am. Chem. Soc. 118*, 4532−4538.
52. Obika, S., Uneda, T., Sugimoto, T., Nanbu, D., Minami, T., Doi, T., and Imanishi, T. (2001) *Bioorg. Med. Chem. 9*, 1001−1011.
53. Leumann, C. J. (2002) *Bioorg. Med. Chem. 10*, 841−854.
54. Mills, M., Arimondo, P. B., Lacroix, L., Garestier, T., Klump, H., and Mergny, J. L. (2002) *Biochemistry 41*, 357−366.
55. Svinarchuk, F., Paoletti, J., and Malvy, C. (1995) *J. Biol. Chem. 270*, 14068−14071.
56. Alunni-Fabbroni, M., Pirulli, D., Manzini, G., and Xodo, L. E. (1996) *Biochemistry 35*, 16361−16369.
57. Sugimoto, N., Wu, P., Hara, H., and Kawamoto, Y. (2001) *Biochemistry 40*, 9396−9405.
58. Rougee, M., Faucon, B., Mergny, J. L., Barcelo, F., Giovannangeli, C., Garestier, T., and Helene, C. (1992) *Biochemistry 31*, 9269−9278.
59. Shindo, H., Torigoe, H., and Sarai, A. (1993) *Biochemistry 32*, 8963−8969.
60. Xodo, L. E. (1995) *Eur. J. Biochem. 228*, 918−926.
61. Porschke, D., and Eigen, M. (1971) *J. Mol. Biol. 62*, 361−381.
62. Prevot-Halter, I., and Leumann, C. J. (1999) *Bioorg. Med. Chem. Lett. 9*, 2657−2660.
63. Gowers, D. M., and Fox, K. R. (1999) *Nucleic Acids Res. 27*, 1569−1577.
64. Verma, S., and Miller, P. S. (1996) *Bioconjugate Chem. 7*, 600−605.

BI025734Y